Research article

Journal of Alzheimer's
Disease Reports
Volume 9: 1–15

DOI: 10.1177/25424823241309664
journals.sagepub.com/home/alr

Repurposing peripheral immunocytes of Bacillus Calmette Guerin-vaccinated melanoma patients to reveal preventive Alzheimer's disease mechanisms, possibly via the unfolded protein response

Benjamin Y Klein[1], Inna Ben-David[2], Ofer N Gofrit[3] and Charles L Greenblatt[1]

Abstract

Background: Alzheimer's disease (AD) dysfunctional unfolded protein response (UPR) is revealed by amyloid-β aggregates. Normally, UPR reacts to endoplasmic reticulum stress by resolving misfolded/aggregated proteins, and UPR failure induces brain-cell apoptosis consistent with AD pathology. Peripheral blood mononuclear cells (PBMC) and immunocyte brain infiltrates are involved in AD pathogenesis, whose risk is lowered by the Bacillus Calmette Guerin (BCG) vaccine. Hypothetically, BCG prevents AD caused by UPR-driven apoptosis in PBMC brain infiltrates, corrected by BCG-vaccinated PBMC brain infiltrates.

Objective: To reveal whether BCG shifts the UPR towards cell survival. Method: PBMC proteins from 6 individuals were compared by immuno-electrophoresis before and after BCG hypervaccination. Cryopreserved PBMC provided an opportunity to analyze the BCG impact on the UPR, although their donor destiny to develop AD was unknown. UPR signaling responsive to BCG was recorded to examine if BCG can influence UPR signaling and thereby explain the previously demonstrated AD prevention by BCG.

Results: UPR signal levels were scored according to positive versus negative cell survival odds by the BCG impact on a dozen UPR signals. The balance between positive and negative scores of individuals emphasizes the impact of the BCG vaccine on the UPR. The antiapoptotic UPR signals under BCG show opposite trends to UPR signals in AD brains, reported by the literature. In conclusion, 3/6 individuals had superior PBMC survival chances under BCG.

Conclusions: These results suggest that the UPR is part of the mechanism responsible for reducing the risk of AD, as previously shown among BCG-treated bladder cancer patients.

Keywords

Alzheimer's disease, Bacillus Calmette Guerin vaccine, capillary-Immunoelectrophoresis, endoplasmic reticulum stress response, peripheral blood mononuclear cells

Received: 15 July 2024; accepted: 5 December 2024

Introduction

Bacillus Calmette Guerin (BCG) is one of the oldest vaccines used in preventive medicine. BCG was introduced in the 1920s[1] and according to the World-BCG Atlas, BCG is used until the present to immunize against tuberculosis. BCG is a potent immunity potentiator and as such it has been used extensively in previous decades (before the use of anti-checkpoint antibodies) to increase the immune response against melanoma tumor-specific antigens (reviewed in[2]). Although intended to serve as an adjuvant, BCG has been implicated as the sole or the main contributor

[1]Department of Microbiology and Molecular Genetics Hebrew University Medical School, Hadassah University Medical School, Ein-Karem, Jerusalem, Israel
[2]Sharett Institute of Oncology, Hadassah University Medical School, Ein-Karem, Jerusalem, Israel
[3]Department of Urology, Hadassah University Medical School, Ein-Karem, Jerusalem, Israel

Corresponding author:
Benjamin Y Klein, Department of Microbiology and Molecular Genetics Hebrew University Medical School, Hadassah University Medical School, Ein-Karem, Jerusalem 91120, Israel.
Email: byklein@mail.huji.ac.il

to the anti-melanoma therapeutic effect[3] and anti-nonmuscle invasive bladder cancer as well.[4] Notably, BCG has non-specific effects on unrelated pathogens, dubbed "off-target effects".[5,6] This phenomenon has been attributed to innate immune training of immunocyte memory exhibited by increasing cytokine secretion after a second challenge by BCG,[7] or by other pathogens. In some instances, the off-target protection effect by BCG may be gender specific.[5,8,9] The training of innate immunocytes may be sustainable for a long time as shown by skin tests in a survey of vaccinated infants,[10] which could be explained by epigenetic imprinting induced by BCG.[11,12] Some of the surprising phenomena of BCG are related to metabolic effects. For example, in insulin-dependent diabetes patients, a long period after being vaccinated with BCG may require a reduction of the insulin dose,[13] which is explained by the conversion of their glucose metabolism from anaerobic to aerobic glycolysis. This is explained by a strongly upregulated blood glucose consumption by the immune system.[13] Another surprising phenomenon is a decreased risk of developing Alzheimer's disease (AD) by exposure to the BCG vaccine.[14] AD is associated with a failure to metabolize microtubule-associated tau-protein aggregates. Experts in stress response ascribe AD to possible disorders of the unfolded protein response (UPR) to endoplasmic-reticulum (ER) stress.[15,16] They aim to therapeutically target the UPR,[15,16] even though the tau protein does not pass through the ER compartment.[17] The tau protein is a leaderless protein skipping the ER and is translocated into the ER-Golgi intermediate compartment; however, the proteins involved in its transport depend on ER quality control.[17] The UPR signaling has been reviewed in general[18] and as related to AD pathology,[19,20] it can be summarized as follows: Part of newly synthesized proteins are normally carried into the ER for quality control. ER chaperones such as immunoglobulin binding protein (BiP) interact with newly synthesized proteins to prevent misfolding. When BiP is outnumbered by excess newcomer ER proteins, the unmatched unfolded proteins compete for BiP molecules, that fix special membranous ER-resident proteins to prevent interaction between monomers in the ER membrane. Loss of BiP unleashes monomers to dimerize, which elicits sensing of unfolded/misfolded stress in the ER accomplished by activation of their cytosolic UPR signaling domains. The important sensors are 1) inositol-required enzyme 1a (IRE1a), 2) activating transcription factor 6 (ATF6), and 3) PKR-like ER-resident kinase (PERK). IRE1a, upon losing its BiP fixer, homodimerizes and auto-phosphorylates in its luminal side. This opens a catalytic endonuclease domain in its cytosolic face that excises 26 nucleotides co-translationally from the mRNA of XBP1u (X box protein 1 un-spliced). This excision results in a frameshift generating a new peptide sequence downstream to the excision by this unconventional splicing (XBP1s). XBP1s is an active transcription factor that transmigrates to its nuclear sites in the nucleus to transcribe BiP mRNA and other genes of the UPR. BiP loss from ER membranous ATF6 precursor starts lateral intramembranous migration of ATF6 toward the Golgi membrane where it undergoes intra-membranous cleavage. The cytosol-facing fragment of ATF6 migrates to the nucleus to act as a transcription factor for BiP, XBP1u, other chaperones, and ER-associated degradation (ERAD) factors, and the rest of its part in the UPR transcription program. The fixative BiP removed from PERK, causes PERK to dimerize and auto-phosphorylate and open a kinase catalytic domain at the cytosolic face to phosphorylate serine51 on eIF2a. Phospho-eIF2a (p-eIF2a) is prevented from joining the eIF2 translation factor complex, thus cap-dependent translation is inhibited. eIF2a acts as an integrating stress response factor by having its serine51 potentially targeted by 3 other different kinases, induced by other different (non-ER stress) cellular stressors.[21] Inhibiting cap-dependent translation provides a chance for BiP and other ER chaperons of the UPR to clear unfolded/misfolded proteins before cap-dependent translation is resumed, this way ER homeostasis is maintained. Here we have a unique opportunity to analyze peripheral mononuclear cells (PBMC) from melanoma patients, before and after they underwent live multiple BCG vaccination rounds. Some of the above-mentioned UPR biomarkers are compared between pre and post-BCG samples by protein expression in PBMC in light of published biomarkers in AD patient brains. The results provide a hypothetical basis for searching mechanisms by which BCG reduces the risk of developing AD.

Methods

PBMC source

PBMC samples were obtained from a cell repository. The committee on research involving human subjects of the Hebrew University-Hadassah Medical School (application 0798-21 HMO, 3rd-year extension up to February 27, 2025) has authorized this research: "deciphering the mechanism by which BCG decreases the risk of Alzheimer's disease". Six patients (Table 1) with various clinical diagnostic statuses of melanoma were treated by vaccination with autologous tumor cell antigens which was accompanied by BCG vaccine that served as an adjuvant, as described in old studies for melanoma at stage III disease.[22,23] The present research is repurposing 7–9 years old cryopreserved samples for exploratory statistically unsupervised learning, seeking to set apart, from a small sample, two groups based on a dozen UPR signaling features that will be sufficiently distinguishable, and reflect clinical results of low versus high-risk AD, compared to a >200-fold larger group presented by reference.[14]

Preparation of the vaccine

The material for immunization was prepared for an old study, (for which patients had to agree by informed

Table 1. Source of PBMC of pre and post-vaccination.

Patient number	1	2	3	4	5	6
Gender	male	male	male	male	Female	male
Age	72	76	63	44	18	70
melanoma	ocular	Skin + lymph node	ocular	skin	Skin + lung	Skin + lymph node
Years cryopreserved	8	9	7	12	9	8
Sampling Interval between pre and post-vaccination	4 months	4 months	4 months	4 months	12 months	4 months

consent via the hospital ethical committee) from resected autologous tumor metastases grown as primary melanocytic cell lines (described in[22,23]). Briefly; tumor cells were grown in culture and identified as melanoma decedents of primary cultures by the expression of S100, MART-1, or gp100 by at least half of the cells and by MHC-class-I related chain. Cells were irradiated (230 Gy) and surface-conjugated with dinitrophenol as previously described[24] to prefer induction of cytotoxic antitumor-specific antigens of the Th1 phenotype. Patients were sensitized to Dinitrophnol 10 days before vaccination. To minimize the activity of suppressor T-regs cyclophosphamide was administered 4 days after the first two vaccination doses.

Vaccination protocol

Cells were injected intradermally $10–25 \times 10^6$ cells per dose. The tumor vaccines were followed by a 1:50 dilution of BCG from the Danish Staten Serum Institute at the first 3 injections and a 1:500 dilution for the next 5 injections. The BCG injections were given at 3-week intervals distantly from tumor locations.

PBMC sampling

A few days before and a week to 10 days after the course of vaccination, coagulation-inhibited venous blood was obtained and separated on a Ficoll density centrifugation 1200xg for 30 min. PBMC at the dilute plasma separated from the Ficoll interphase were washed in cold growth medium and suspended in cold dimethyl sulfoxide and 20% cold fetal calf serum (FCS) and gradually frozen to negative – 170°C, to be kept in liquid nitrogen until further use for the old original study.[22]

Thawing of PBMC and protein extraction

Years later for the present repurposing study, cells in frozen vials were rapidly thawed in a water bath at room temperature until the frozen suspension reached 0°C. Cells were diluted in 20 volumes of cold Dulbecco phosphate-buffered saline (PBS) 2% FCS, spun 10 min, 300xg at 4°C, and washed twice in ice-cold plain PBS to remove all cryopreservation solution and FCS traces. The cell pellets were suspended in a 200 µl ice-cold Bicine/CHAPS detergent lysis buffer kit (CBS 403) with inhibitors of proteases and phosphatases (Protein Simple San Jose, CA) designed to minimize nuclear lysis. The cell suspension was incubated on ice 30 min and spun for 30 min at 10000 x g at 4°C. Supernatants of proteins were frozen at −20°C until further use.

Preparation of immuno-electrophoresis samples

Samples were prepared using a separation module kit for a molecular weight range of 12–230 MW for a 25 capillaries cartridge (SM-W004) good to be used on an Abby instrument (see Protein Simple website for the Abby instrument). A master-mix solution was prepared according to the producer's instructions using a standard pack from the kit that provides dithiothreitol, a proprietary master mix compound, and a 5x concentrated sample buffer. The ready-to-use master mix was prepared such that per one capillary a 0.6 µl master mix is to be added to 2.4 µl of protein solution (total volume/sample =3 µl, with 0.8 µg protein), boiled at 95°C for 5 min and loaded on a producer-designed plate in a row of 24 wells for the samples, and 1 well for the supplied biotinylated molecular weight ladder. The detection module (mostly DM-001 [anti rabbit]) of the kit contained the second antibody HRP conjugate, the antibody diluent which serves also as a blocking buffer, the luminol, and hydrogen peroxide. The rest of the separation module of the kit contains a wash buffer, plates, and capillary cartridges. We used a total-protein detection module (DM-TP01) in a RePlex format in which after the regular immune electrophoresis the antibodies undergo in-capillary stripping and a special catalytic reagent biotinylated the total capillary proteins (in-capillary) that are then detected by streptavidin. The first antibodies are purchased separately from other suppliers. From the loading of the plate onto the instrument to the end of the procedure all the described electrophoretic and catalytic steps are automatically performed and computer-recorded, without human intervention.

Antibodies

Anti PERK rabbit monoclonal antibodies (R-mAb) from Cell Signaling Technology (CST) Catalog No (#) 3192,

anti-phospho-PERK pThr980 R-mAb CST #3179, anti-IRE1a R-mAb CST #3294, anti-phospho-IRE1a p-S724 R-polyclonal Ab Novus Biologicals (NB) #NB100-2323, anti-BiP R-mAb CST #3177, anti GAPDH R-mAb XP CST #5174, anti eIF2a mouse-mAb CST #2103, anti-phospho-eIF2a Ser51 R-mAb CST #9721, anti ATF6 R-polyclonal Ab NB #NBP1-75478, anti XBP1 R-polyclonal Ab NB #NBP1-77681. Antibodies were diluted 1:100 in the diluent solution provided in the detection module of the electrophoresis kit (Protein Simple).

Analysis

The Abby instrument provided results by recording chemiluminescent signals of secondary antibodies directly from the capillaries at the last stage of the automated runs. The antigen peak quantities are kept in records in the run files as arbitrary numbers. For readers acquainted with the old Western blot methodology, the instrument may opt to translate the original reading from the capillaries into virtual bands. Importantly, this is the opposite of Westen blot records, where the bands on nitrocellulose blots constitute the original chemiluminescent signals. The original signals from the run files are presented in Supplemental Table 1 and are the original chemiluminescent results. The counts of the total protein along the capillary are recorded by the instrument and were copied into an Excel file to obtain a summation of all total protein per capillary to which antigen peaks from respective samples in capillaries are related.

Presentation of the results

The arbitrary antigen peak quantities are presented mostly as a fraction of the total protein chemiluminescent signals, obtained in arbitrary numbers, as detected by the Abby instrument. These relative antigens (signaling proteins) abundance is presented per patient, as pre versus post-BCG treatment course. The illustration is either by comparative bar graphs or linear or other regression in which the regression lines contain pre-BCG results in blue versus post-BCG results in red. The dots are designated by individual patient numbers. The correlation coefficients of each regression are provided by PowerPoint software and its statistical significance is computed via SPSS. The regression lines express the relation between enzymes on the X axis and expected responding protein substrates on the Y axis. The difference between opposite regression trajectories is tested by Fisher's z transformation. On top of some regression lines, the effect of the BCG-reinforced vaccine course is overlaid by an arrow (up or downwards) in red for the (Y-axis) substrate or responding protein, and in horizontal blue for the (X-axis) enzyme or activation protein. Each pair of red-blue arrows represents a respective patient number. A summary table of up down effect of BCG is presented separately for all detected antigens. For each signaling protein, a positive (+) or negative (−) score is added. The difference between pre and post-BCG is expressed as the percent fraction of the larger result. If the pre-BCG is bigger than the post-BCG abundance the percent loss is presented as a negative value, otherwise it is expressed as a positive value. The scores of each patient are recorded in the bottom rows.

Results

PBMC from six individuals vaccinated with dead (irradiated) melanoma antigens reinforced by live BCG as an adjuvant. Proteins extracted from isolated PBMC, before and after the vaccination course, were compared by immune-electrophoresis. This is a statistical unsupervised survey for the development of hypotheses about the mechanism/s by which vaccination has protected individuals against the risk of developing AD.[14] The basic assumption is that peripheral immunocytes that gain access to the brain may possess transmissible factors or provide cell surface cues that protect neurons and nonneuronal cells (microglia and astroglia) against neurodegeneration.[25] Because one of the hallmarks of some neurodegenerative diseases consists of protein aggregation, e.g., prions, amyloid-β, and tau protein although the latter is not exposed to the ER, we chose to examine the proteins involved in the prevention of aggregate formation and clearing misfolded proteins, i.e., the ER stress response.[26,27] Among the three sensors of ER stress, PERK, ATF6, and IRE1a, PERK is the sensor that immediately reacts to ER protein misfolding and aggregation by shutting off cap-dependent translation as a start.

PERK response to vaccination

PERK is normally activated when the ER lumen is overloaded by unfolded or misfolded newly synthesized peptides.[28] PERK auto-phosphorylates at its ER luminal domain which activates its cytoplasmic domain kinase that in turn phosphorylates the S^{51} residue of the alpha component (eIF2a) of the eIF2 translation complex. This generates p-eIF2a which inhibits cap-dependent translation by the eIF2 translation initiation complex.[29] Figure 1(a) shows the virtual band density representing the immunoreactivity of the active phosphorylated PERK dimer (p-PERK) and the panel below shows the bands of inactive PERK monomer. Figure 1(b) shows two point-scatters one plotted ratio between the phosphorylated active PERK (p-PERK) dimer and its inactive monomer PERK (X-axis) against its catalyzed substrate p-eIF2a ratio to eIF2a (Y axis) of PBMC before BCG vaccination, and the second

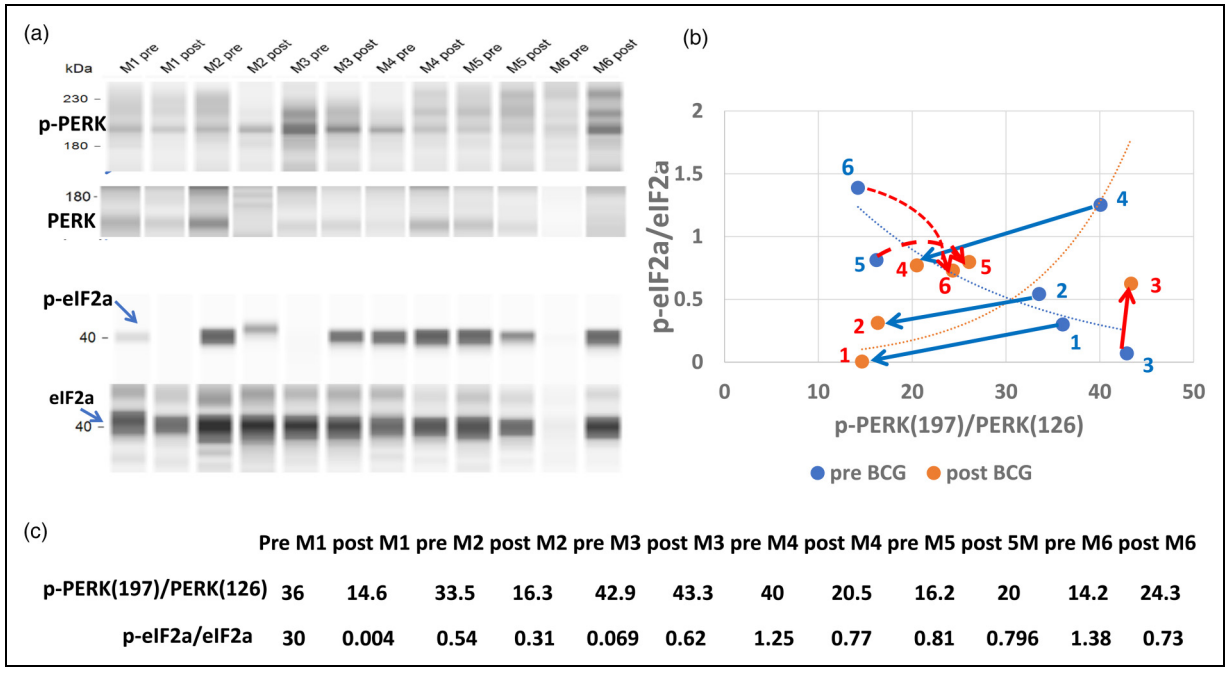

Figure 1. Activated PERK (p-PERK) targeted substrate (eIF2a) matched with resulting p-eIF2a: after vaccination, patients 1, 2, and 5 show a decrease in activated kinase (p-PERK) congruent with a decrease in its phosphorylated substrate p-eIF2a (blue arrows). In contrast, patients 3, 4, and 6 show an increase in p-eIF2a (red arrows), accompanied by a decrease, or no change, or increase in p-PERK in patients 3, 4, and 6, respectively.

after vaccination of each of the 6 patients. In patients 1, 2, and 4, p-PERK is downregulated and in patients 3, 5, and 6 p-PERK is upregulated after the course of vaccination. The response of p-eIF2a in 1, 2, and 4, is in congruence with the p-PERK reduction while in 3, 5, and 6 responses are unrelated to p-PERK changes. This incongruence may be due to any of 3 other kinases (specific for different stress conditions[21]), or due to a negative response to specific phosphatases[30] that fail to hydrolyze p-eIF2a.

Expression of BCL2A1 versus p-PERK

Because activation of PERK results in translation shutdown via inactivation of eIF2a, PERK activation was tested in association with the levels of A1 cell-survival protein. Figure 2(a) illustrates the PBMC levels of A1 before and after vaccination, side by side with the levels of p-PERK from the samples of the same patients (Figure 2(b)). Comparing both bar graphs gives the impression that the figures seem inversely related between patients, which is confirmed by the scatter graph (Figure 2(c)) by an exponential best fit ($p = 0.00031$). This implies that under an extensive vaccination schedule with BCG, A1 expression is decreased while that of p-PERK is increased, in contrast to the pre-vaccination status. Still, at low p-PERK, some A1 are expressed at higher levels.BCL2A1 is an antiapoptotic paralog of the antiapoptotic protein BCL2 highly expressed in PBMC with some diffuse expression in areas of the brain.[31] As shown previously,[32] BCG stimulates A1 expression more extensively than that of the canonical BCL2 expression (compare the Y axis in Figure 3(b) with (a)). A1 was upregulated by BCG in patients 1, 2, 4, and 5 and downregulated in 3 and 6. Patients 1, 2, 3, and 6 showed an opposite trajectory versus the canonical BCL2 in which the scale was much smaller than that of A1. Figure 3(c) illustrates the immunoelectrophoretic bands of BCL2 and A1 appended by their ratios to total proteins.

CHOP response to vaccination

CHOP (C/EBP homolog) acts as a dominant negative transcription factor competing against the C/EBP transcription factor by binding to its promoter cis-elements[33] and as such CHOP serves to promote the expression of proapoptotic proteins.[34] Upon chronic PERK activation that is followed by chronic eIF2a inactivation. ATF4 (activated transcription factor 4) and CHOP are known to be upregulated as is CHOP in Supplemental Figure 1, this may occur during ER stress due to unresolvable protein misfolding. This cascade can lead to the expression of proapoptotic death proteins and cell death[34] as in AD brains. Here in patients 1, 3, and 5, CHOP is upregulated in post-vaccinated PBMC, although p-PERK is downregulated (Figure 3(a) and (b), versus Figure 1). In patients 1 and 5, CHOP

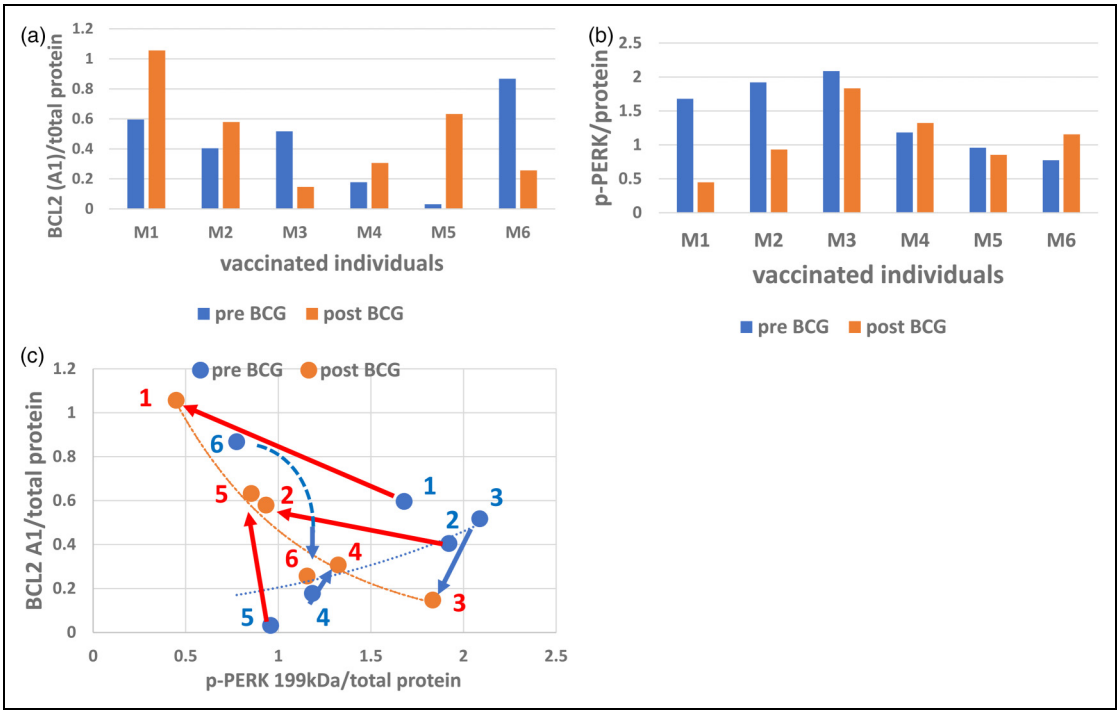

Figure 2. BCG decreases activated translation inhibitor (p-PERK) inversely to increase the survival factor BCL2-A1: the BCL2 A1 isoform was upregulated in PBMC after vaccination in patients 1, 2, 4, and 5, phosphorylation-activated state (p-PERK) is conversely downregulated in patients 1, 2, slightly in 5, and runs inversely in 6, and 3 (b). The bar graphs in (a) and (b) make an inverse impression by eye bolling and when plotted (c) show inverse regression curves with an exponential best fit The pre-BCG curve (blue dots) has a positive correlation coefficient ($r = 0.3601$, $n = 6$) but is insignificant ($p = 0.241$) whereas the post-BCG negative curve ($r = -0.966$, red dots) is significant ($p = 0.0008$) and the difference between these opposing curves, tested by the Fisher's z transformation, is highly significant ($z = 2.959$, $p = 0.00031$).

increase is accompanied by the antiapoptotic BCL2A1 upregulation, but not in patient 3 in which the eIF2a did not recuperate from its inhibited p-eIF2a status. This may indicate that the mechanism through which p-PERK is downregulated by vaccination did not relieve the phosphorylated S^{51} which could have been induced by at least one of the 3 other stress-responsive kinases that target eIF2a S^{51} as well.[35] Patient 6 is exceptional by having p-PERK and its p-eIF2a substrate upregulated by vaccination (only when related to total protein) while the pro and antiapoptotic proteins CHOP and BCL2A1 respectively, are both downregulated. When related to the total PERK and total eIF2a the p-eIF2a is more downregulated than p-PERK (Figure 1) possibly due to the overactivation of the p-eIF2a targeting phosphtase.

ATF6 transcription factor response to vaccination

Activated transcription factor 6 (ATF6) is the 2nd stress sensor embedded in the ER membrane. Once ER stress ensues ATF6 in its precursor form is cleaved by an intramembranous catalysis to release the cytosol-facing fragment ATF6(N) (ATF6 nuclear). ATF69(N) is trafficked to the nucleus where it acts as a transcription factor at its designated transcription program.[36] In relevance to the UPR, ATF6 promotes transcription of ER-resident chaperone genes among them the BiP mRNA and transcription factor XPB1 mRNA[37] that is designated for cytosolic unconventional splicing by a third ER-resident stress-sensing enzyme IRE1.[18] The co-translationally spliced XBP1 (XBP1s) mRNA becomes a transcription factor protein, that transactivates chaperone genes in addition to similar partially overlapping activity performed by ATF6(N). The protein expression of XBP1s is dependent on that of ATF6(N) which requires a substantial time lag by which ATF6(N) synthesis predates that of XBP1s.[38] This phenomenon may be reflected by a particular dot scatter in Figure 4, which illustrates 5 panels. Figure 4(a)–(c) show the ATF6 precursor (81 kDa), the ATF6(N) transcription factor, and the glycolytic enzyme GAPDH, respectively, all depicting the pre and post-vaccination results. Figure 4(d) and (e) show dot scatters where XBP1s protein (Y axis) represents the presence along ATF6 precursor activation (X-axis, Figure 4(d)), and its response to ATF6(N) transcription factor in Figure 4(e). The post-BCG of patients 1 and 2 (red) dots reach over a far distance from the pre-BCG respective

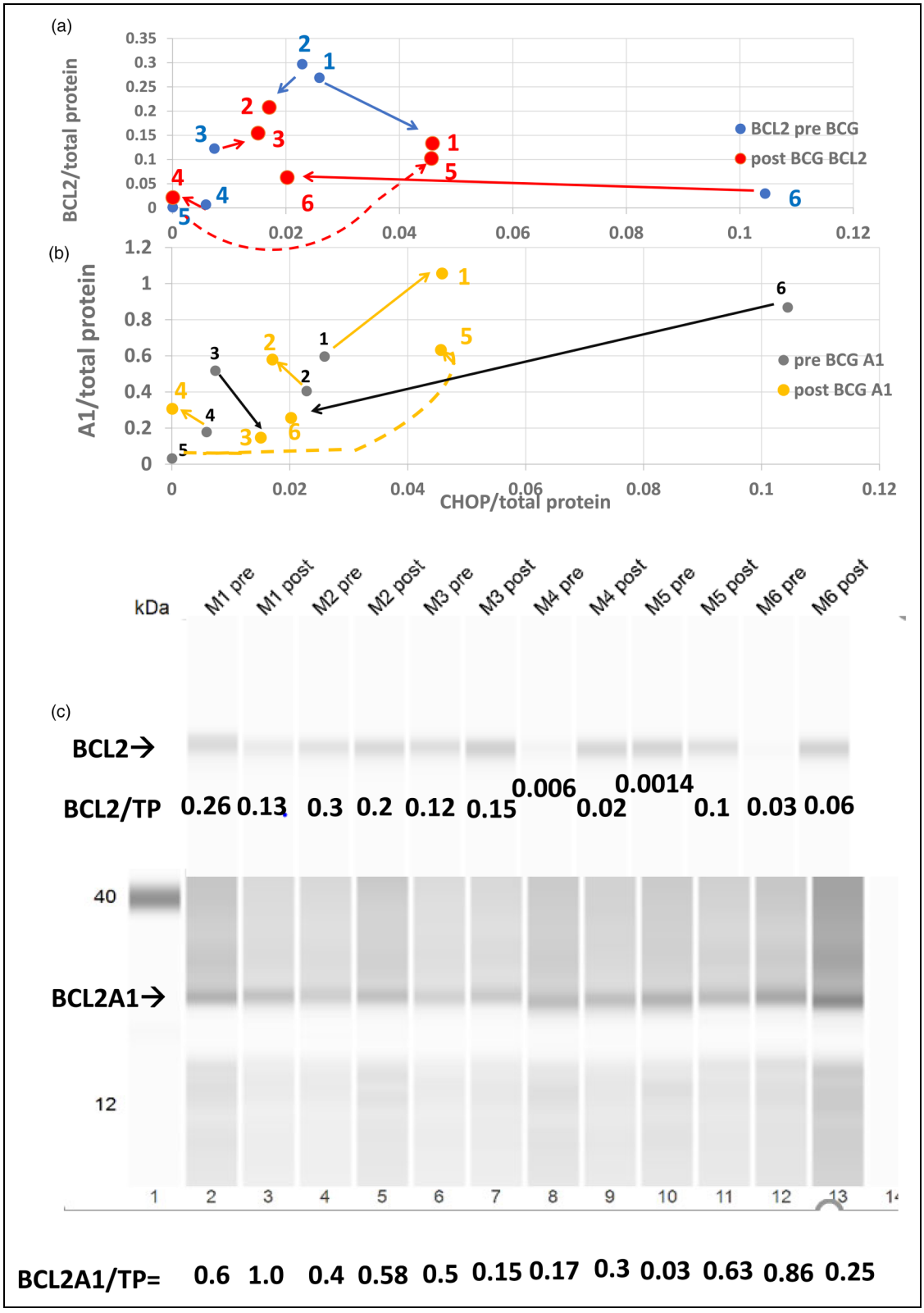

Figure 3. BCG vaccine differential impact on BCL2 and its A1-related survival protein: BCL2 survival protein (a) shows lower response to apoptosis-inducing CHOP transcription factor than the A1-related BCL2 survival factor (b) under BCG: BCG increased the A1 BCL2 related cell survival factor (b) responses in patients 1, 2, 4, and 5 against proapoptotic CHOP in contrast to canonical BCL2 (a). BCL2 electrophoretic virtual bands of pre and post-BCG vaccination are shown above the A1 BCL2 related bands (c) accompanied by their concentration relative to total protein (TP).

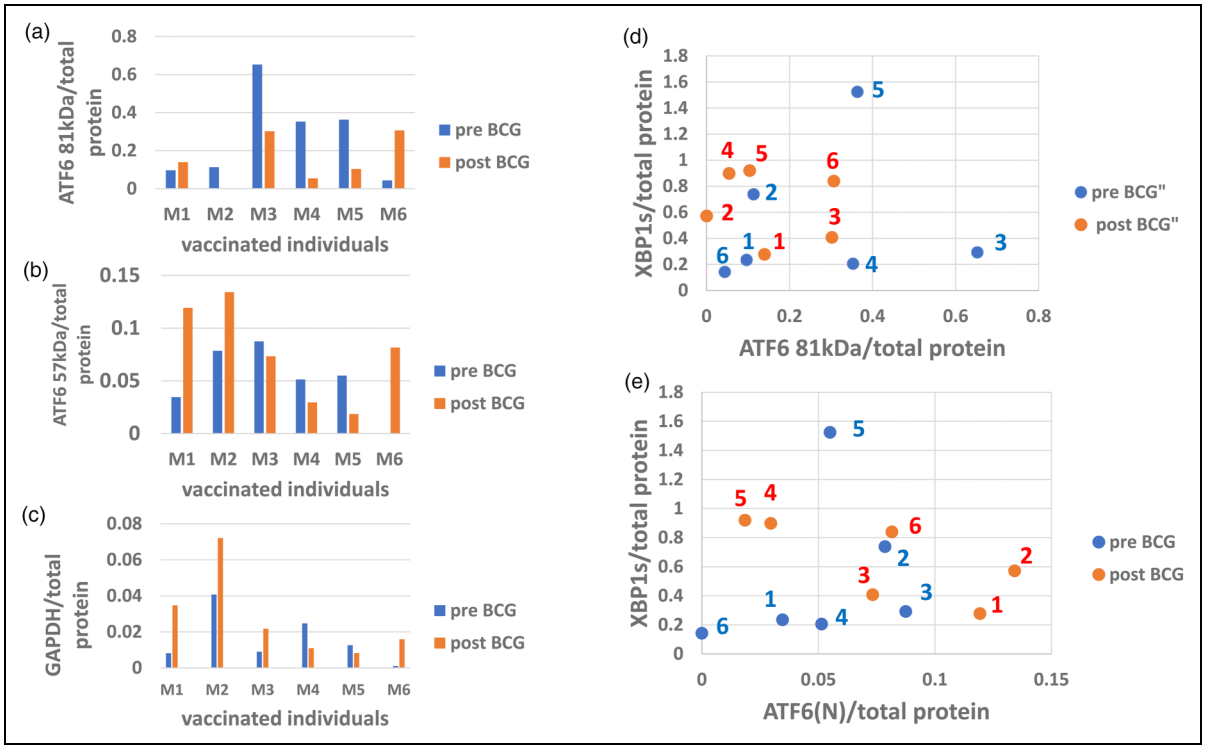

Figure 4. ATF6 and XBP1s activated protein abundance in PBMC after vaccination: ATF6 transcription factor precursor abundance before (blue) and after (red) vaccination (a) and its derivative activated transcription factor ATF6(N) (b) were detected by immuno-electrophoresis. The pattern of BCG vaccination effect on ATF6 activation relative to pre-BCG (b) is similar to that illustrated by the GAPDH effect (c) in 5 out of 6 patients, apart from patient 3. Note the vaccination effect in patient 2 where close to 100% of the ATF6 precursor (a) was consumed to generate the active ATF6 57 kDa (ATF6(N) isoform (b, d, e). The quantitative relationship between the ATF6 precursor versus XBP1s for individual patients before and after vaccination is shown in (d) and that of the activated (ATF6(N)) versus XBP1s is shown in (e).

(blue) dots parallel to the ATF6(N) X axis whereas in parallel to the XBP1s Y axis, there is hardly any distance for patient 1 and even a slight reduction for patient 2. We interpret this presentation as a vaccination-induced low XBP1s abundance or slow synthesis versus an increase in ATF6(N) abundance or faster synthesis. The low abundance may be explained firstly by the loss of XBP1s to heterodimerization with ATF6(N) fulfilling a catalytic function,[38] and/or secondly by the substantial prolonged time of XBP1s synthesis lagging behind the faster synthesis and processing of ATF6(N), starting from the moment of stress sensing.[38] The heterodimerization can be supported by the increase in GAPDH (Figure 4(c)) in patients 1 and 2 parallel to the changes in patients 1 and 2 in Figure 4(b) and (e). A possible explanation for this argument is that both XBP1s and ATF6 may induce transcription of ERAD factors to resolve misfolding in the ER. However, heterodimers between these two transcription factors are by far more efficient than when working separately, the parallel increase in glycolysis (GAPDH up in patients 1 and 2) may reflect the higher requirement of energy for the execution of ERAD functions.[38] BCG is known to be responsible for the reprogramming of anaerobic to aerobic glycolysis in immunocytes.[13,39,40]

IRE1a response to vaccination

Transcription of the XBP1 gene into its mRNA by ATF6(N)[37] is followed by IRE1a, which processes XBP1u (un-spliced) mRNA.[41] It requires IRE1a dimerization for autophosphorylation at the ER luminal side to open the RNA endonuclease domain on its cytosolic side to be activated (becoming p-IRE1a). Figure 5 shows a matching between activated enzymes p-IRE1a 107 kDa (5A) or p-IRE1a 135 kDa (5B) with the resulting expression of spliced XBP1s protein product. Figure 5(c) is appended below and shows the p-IRE1a and XBP1s virtual bands and the per-total protein density. Activated p-IRE1a 107 kDa is up in patients 1 and 3, slightly up in 4 and 6, and down in patients 2 and 5 (Table 2, line 10). The 135 kDa p-IRE1a isoform has a different distribution (Figure 5(b) and Table 2, line 11), but more impressive is the X-axis scale in Figure 5(b) which is by one order of magnitude higher than it is for the 107 kDa.Thus, the same level

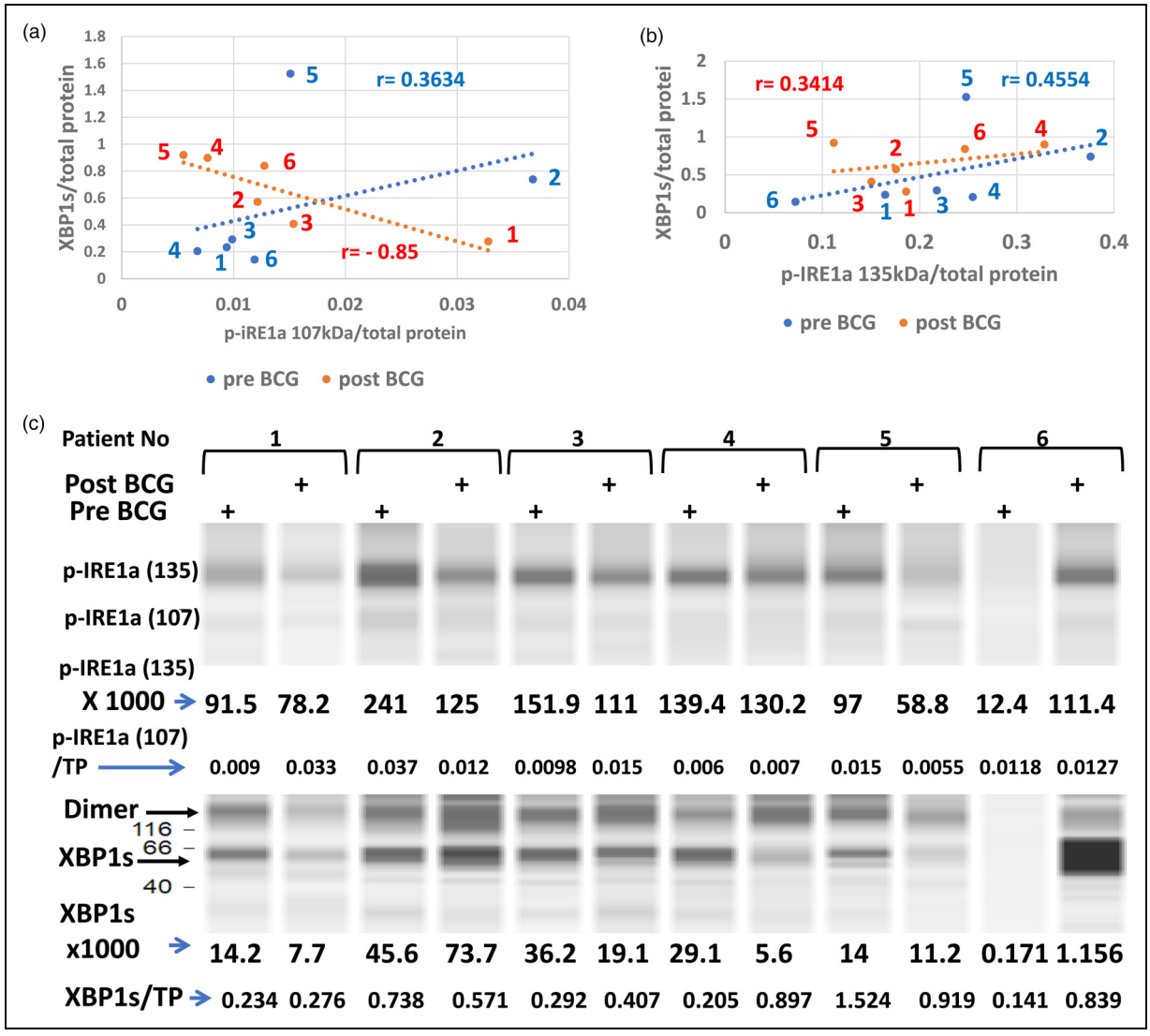

Figure 5. Levels of activated (spliced) XBP1s versus its activated stress sensor p-IRE1a by vaccination: the phosphorylation-activated ER-stress sensor p-IRE1a from PBMC of 6 patients before (blue) versus after the course of vaccinations (red) is presented against its activated substrate XBP1s. Two p-IRE1a isoforms are presented; 107 kDa (a) and 135 kDa (b), against pre and post BCG levels of XBP1s. The protein levels of each patient are marked by their numbers and the correlation coefficients before (blue) and after vaccination (red). Note that XBP1s molecules are concentrated above the low p-IREa 107 kDa levels (a), contrarily to the 135 kDa isoform where the same XBP1s concentrations are spread over levels that span between one half to one and a half orders of magnitude of the activating enzyme. Under low levels of the stress sensor (p-IRE1a), BCG vaccination changes the relations to XBP1 response and the difference between regression lines tested by Fisher's z transformation test is significant ($p = 0.045$, $n = 6$)—abundance of activated IRE1a (p-IRE1a) and its enzymatic reaction product XBP1s in PBMC (c). Immuno-electrophoresis of PBMC protein extracts from the 6 melanoma patients before versus after anti-autologous tumor vaccination reinforced by the BCG adjuvant are presented. The virtual band of p-IRE1a (135 kDa) numbers of arbitrary abundance is accompanied by those of XBP1s from identical samples shown below. A smaller size p-IRE1a (107 kDa) of much lower density is presented as a fraction of total protein (p-IRE1a/TP).

of XBP1s response requires on average a 10fold higher stimulus (or dosage) by the p-IRE1a 135 kDa than by the 107 kDa isoform. This may mean that the former is functionally attenuated. The attenuated 135 kDa p-IRE1a molecular size is larger than the 107 kDa isoform which may reflect a fusion of 107 kDa molecule with a J-protein (28 kDa ERdj4) cochaperone. Normally this occurs upon subsiding of the ER stress when the J-protein interacts with the p-IRE1a dimer to activate an available BiP molecule by its ATP to bind BiP to the p-IRE1a dimer and disrupt the dimer into monomers.[42]

Bip response to XBP1s

Transcription of the BiP gene can be activated by ATF6(N) or by XBP1s, BiP mRNA is mainly translated during ER

Table 2. Impact of vaccination reinforced by BCG on UPR in PBMC.

		Patient number						
line	Signaling proteins	1	2	3	4	5	6	Published effects in the brain
1	p-PERK	Down (−58.4)	Down (−51.3)	Up (+0.4)	Down (−48.7)	Down (−19)	Up (+41.5)	Pro-AD, when chronically high[15,26,27,43]
2	p-eIF2a	Down (−98.6)	Down (−42.6)	Up (+88.8)	Down (−38.4)	Down (−2.4)	Down (−47.1)	Pro AD when chronically high[44–46]
3	BCL2A1	Up (+40)	Up (+31)	Down (−70)	Up (+43.3)	Up (+95.2)	Down (−70.9)	Antiapoptotic, antagonizing CHOP?[32]
4	BCL-2	(−50)	(−33.3)	(+20)	(+70)	(+98.6)	(+50)	
5	CHOP	Up (+44.4)	Down (−26)	Up (+53.3)	Down (−98.8)	Up (+99.8)	Down (−80)	Proapoptotic if persistently high[45,47]
6	ATF6 precursor	Up (+30.9)	Down (−99.6)	Down (−53.6)	Down (84.7)	Down (−71.3)	Up (+85.6)	Alert for ER stress[48]
7	Activated ATF6	Up (+71.4)	Up (+41.8)	Down (−16)	Down (−41)	Down (−66.6)	Up (+99.9)	Transcribes BiP, XBP1[48] and ERAD, ER chaperones
8	XBP1s	Up (+5)	Down (−55.5)	Up (+28.4)	Up (+78.7)	Down (−20)	Up (+75.9)	Transcribe BiP, ERAD as heterodimer with ATF6[48]
9	GAPDH	Up (+97.6)	Up (+44.4)	Up (+40)	Down (−48.3)	Down (−33.3)	Up (+93.3)	Glycolytic intensively by BCG[13,49,50]
10	p-IRE1a 107 kDa	Up (+71.8)	Down (−66.6)	Up (+40)	Up (+14.2)	Down (−66.6)	Up (+8.3)	p-IRE1a dimer activates XBP1[48]
11	p-IRE1a 135 kDa	Up (+11.8)	Down (−53.3)	Down (−30.8)	Up (+19.5)	Down (−55)	Up (+70)	XBP1 activation attenuated by p-IRE1a[42]
12	BiP	Up (+60)	Down (−5.2)	Down (−9)	Up (+40)	Up (+26.6)	Up (+20)	Inhibits misfolding, and keeps ER stress sensing alert[27,28,45]
14	Pro-AD	−113.6	−119.9	+142.5	−185.9	+78.4	−109.4	Odds of apoptosis by BCG
15	Anti-AD	+338.5	−196.4	−50.4	+81.7	−92.4	+432.9	Odds of anti-apoptosis
15	Final score	+452.1	−76.4	−192.9	+267.6	−170.8	+542.3	A sum of PBMC survival odds by BCG-induced UPR

stress when eIF2a is inhibited, but since its translation is cap-independent BiP expression is not inhibited.[51] Figure 6 shows the response of BiP (Y-axis) to XBP1s (X-axis). BiP is upregulated in patient 1 without any change exhibited by XBP1s, and in Patient 5 it is upregulated while XBP1s is downregulated, only the limited BiP increase in patients 4 and 6 can be credited to XBP1s for having contributed its transcriptional support, for patients 1 and 6 ATF6(N) might have been responsible for transcription of the BiP gene.

Discussion

The impact of Vaccination on the UPR pathway is likely to reflect the fraction of individuals that had been protected, or gained a delay, against AD development, according to several published results. The successful protection against AD was anywhere between 20 to 60% better than control patients of the studied populations.[52–55] Therefore, in light of population heterogeneity, it is expected that changes caused by vaccination in the 6 presently analyzed patients, will show reasonable features caused by the vaccines in 1 to 3 patients out of 6 which may explain an anti-AD effect without subjecting this patient to specific cognitive tests. Table 2 reveals the heterogeneity of the BCG effect on the UPR response reflected by a matrix of 6 patients X 12 UPR proteins. The extreme of the heterogeneity is seen in CHOP (Supplemental Figure 1). In Table 2, each point represents a loss (negative) or gain (positive) of protein abundance induced by the vaccine. For the 3 potential proapoptotic proteins (p-PERK, p-eIF2a, and CHOP) gain was subtracted from the total antiapoptotic balance, and loss was added to it. The bottom line shows that patients 1, 4, and 6 had a net positive antiapoptotic balance and 2, 3, and 5 had a negative balance, and according to this scoring approach, the PBMC of 3 BCG vaccinated patients out of 6 show a substantial positive cell survival chance versus the rest that show negative scores. To discuss the heterogeneity of this UPR analysis results one patient can be used, and compared to the rest. For example, patient 1. Vaccination of patient 1 has cut the level of p-PERK (line 1) by more than one-half and its substrate (line 2) (inhibited eIF2a [p-eIF2a]) has shown an even stronger reduction. This branch of the UPR can potentially activate ATF4 and further downstream the proapoptotic CHOP, which has indeed increased (line 5), making the downregulation of p-PERK and p-eIF2a a reasonable positive reaction induced by the vaccine. The increase in the antiapoptotic BCL2A1 protein (line 3) is also a reasonable counteraction to the increased CHOP (line 5) expression, for which the vaccination can be credited.[32] Note that in some tauopathies a low PERK function causes tau protein aggregation in which the low PERK results from PERK hypomorphs due to nuclear polymorphism.[56] This however differs from the present case in which

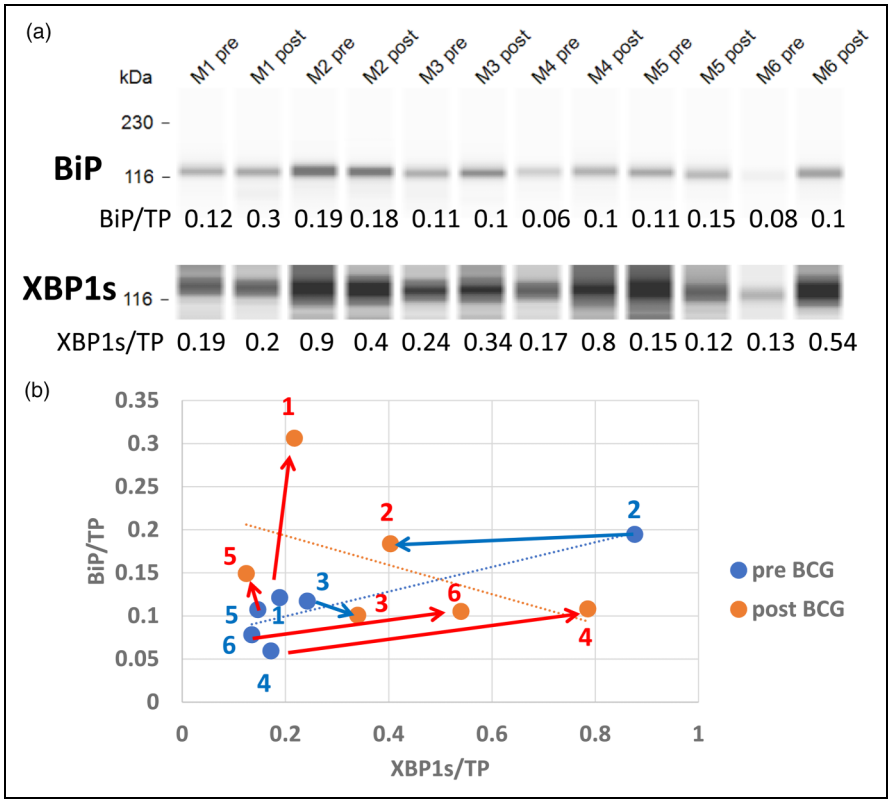

Figure 6. Vaccination impact on the abundance of XBP1s transcription factor and its target gene product, the BiP protein: XBP1s and BiP proteins (a) detected by immunoelectrophoresis from 6 patients before and after vaccination courses, are shown above their ratio to total protein (TP) per capillary. Each XBP1s concentration is matched with the respective BiP concentration on a scatter graph (b). The effect of BCG vaccination is depicted in red dots and their effects directions in red arrows drawn from pre-vaccination blue dots. Blue arrows denote the reduction of BiP. The positive linear regression of individuals before vaccination is in the opposite direction to the regression line of their respective values after vaccination. The correlation coefficient before vaccination is ($r = 0.8844$) opposite to the post-vaccination negative coefficient, $r = -0.5092$ ($n = 6$ for both). The difference between these coefficients tested by Fisher's Z transformation is significant ($Z = 2.39$, $p = 0.016$).

BCG has reduced p-PERK expression from a higher level seen at the pre-BCG vaccination in PBMC (Figure 1(b)). ER, membranous ATF6 was upregulated (Table 2, line 6) and so was XBP1s (Table 2, line 8). The ATF6(N) transcription factor activated by cleavage (line 7) was also upregulated by the vaccination. Interestingly, vaccination has increased GAPDH expression in the same patient (line 9) which is consistent with an increase in available glycolytic energy (ATP). The ability of vaccination to convert anaerobic to aerobic glycolysis was shown by others who have used the BCG vaccine in insulin-dependent diabetes,[13] and by innate immune cells training.[57] Increased ATP production rate can be utilized by ERAD molecules to degrade stress-induced misfolded proteins for which heterodimers of ATF6(N)+XBP1 may serve as transcription factors by far more potent when co-activated[38] versus ATF6(N) or XBP1s when separately active. IRE1a activated to p-IRE1a of 107 kDa is upregulated (Table 2, line 10) by vaccination and has a robust positive role in the activation (by unconventional splicing) of XBP1 mRNA to become XBP1s protein (lines 8). The p-IRE1a 107 kDa is likely the monomer derived from the activated dimer by the conditions of sample preparation. The p-IRE1a 135 kDa (Table 2, line 11) demonstrated a weaker XBP1s activation capacity by one order of magnitude than the same XBP1s activation capacity shown by 107 kDa isoform (compare the X axis of Figure 5(a) to (b)). Vaccination has slightly increased the 135 kDa molecule that strongly attenuated XBP1s activation, therefore it has achieved a lower score than 107 kDa. The explanation for the additional 28 kDa of the attenuated p-IRE1a isoform could be an intermediate stage in which the J-protein (ERjd4) is responsible for attaching the BiP molecule to p-IRE1a that keeps IRE1a as an inactive monomer.[42] Perhaps this p-IRE1a 135 kDa molecule was caught by the sample preparation condition while it was still phosphorylated and attached to the ERjd4 protein. BiP was strongly upregulated in patient 1 (Table 2, line 12) by vaccination indicating a positive UPR and antiapoptotic activation. According to the scoring rationale described above for patient 1, the rest of

the 5 patients are evaluated. The positive scores are summed in Table 2, line 13, for the summation of the pro-apoptotic, and in Line 14 the anti-apoptotic scores are presented, and in Table 2, line 15, the final balance of the survival chance of PBMC of each patient is presented. There are limitations to the ability to interpret the results: firstly the size of the experimental sample is too small although it is a longitudinal study in which each patient presents its control, and therefore it does not require age and gender matching. One of the persons was relatively young (18Y) and the only female, which may add to the diversity of the results, this can be seen according to studies in animal models in which animals are grouped by age. For example, conditional ablation of the endonuclease at the cytosol domain of p-IRE1a exhibited behavioral changes consistent with neurodegeneration in old age[44] that in the young such changes have not been observed. The authors interpreted it as a compensation capacity related to young age, perhaps based on p-IRE1a functions beyond the utilization of the endonuclease. In addition, whatever we find in the UPR of PBMC does not guarantee to look the same in brain tissue. Remarkably in patient 2, the ATF6 precursor seems maximally consumed and not recovered despite p-PERK and p-eIF2a being downregulated and should not inhibit ATF6 translation. XBP1s in patient 2 is also low and is the BiP protein product of its gene target. BiP protein normally fixes ATF6 to the ER membrane, and when low ATF6 is cleaved to produce ATF6(N) which may be part of the reason for the very low ATF6, but perhaps insufficient to explain it, ATF6 translation may be inhibited by microRNA for unknown reason. Patient 6 PBMC are exceptional by their high antiapoptotic UPR signals, although p-PERK is upregulated its substrate p-eIF2a is downregulated which explains why the downstream CHOP is also downregulated. The reason for the seemingly low p-eIF2a response to p-PERK could be overexpression (for unknown reason) of the phosphatase that negatively controls the p-eIF2a.

The prevention or delay of AD pathogenesis is a major problem because it requires the maintenance of persistent healthy behavior and if pharmacological means are available (that are not causing epigenetic imprinting) they will require maintenance as well. The finding that some vaccines (especially BCG) reduce the risk of AD should be embraced, firstly because clinically BCG does not require maintenance. Secondly, it can be used by ex vivo PBMC to follow the signaling mechanism of activity in peripheral blood immunocytes, before looking at the brain tissue that poses an ethical problem in humans. The characteristic neurodegeneration results from human brains are mentioned in Table 2 with proper references published by others, they show mostly opposite results to those in the PBMC of patients from the present work. The fraction 3/6 of them, 50% is close to the 58% of censored results from the retrospective study.[14] What is yet missing are the upstream points of the BCG vaccine impact, necessary and sufficient to induce the UPR or other changes to achieve AD prevention. Interestingly, BCG vaccination can cause emergency granulopoiesis[58] which causes massive outbursts of neutrophils and secretion of granulocyte-colony stimulation factor (G-CSF). A pilot experiment on 8 humans suggested that administration of G-CSF improves cognitive functions.[59] Others have repurposed the administration of G-CSF on 12 humans and found improved scores on cognitive tests.[60] These findings await cognitive testing on larger experimental groups. Notably, as BCG induces an epigenetic signature on histone lysine moieties, G-CSF that responds to the BCG vaccination may be responsible for these particular methylations. Methyltransferases are likely activated by stimulation of the G-CSF receptor expressed by myeloid progenitors,[61] which are perhaps responsible for the long-term sustainability of the BCG vaccination. Within the transcription program of genes remodeled by this receptor stimulation, there may be those that are relevant to the protection of brain tissue for which BCG is responsible for AD prevention. These may include some of the UPR genes.

Acknowledgments

We thank Professor Michal Lotem for her help. Grammar and syntax were corrected using the Grammarly program.

ORCID iD

Benjamin Y Klein https://orcid.org/0009-0002-2730-6395

Statements and declarations

Author contributions

Benjamin Y Klein (Conceptualization; Formal analysis; Funding acquisition; Investigation; Methodology; Writing – original draft); Inna Ben-David (Methodology); Ofer N Gofrit (Funding acquisition; Methodology; Project administration; Writing – review & editing); Charles L Greenblatt (Conceptualization; Formal analysis; Funding acquisition; Investigation; Project administration; Supervision; Writing – review & editing).

Declaration of conflicting interests

The authors declared no potential conflicts of interest with respect to the research, authorship, and/or publication of this article.

Funding

The authors disclosed receipt of the following financial support for the research, authorship, and/or publication of this article: This work was supported by CureAlz, Cure-Alzheimer's Disease Fund.

Data availability

The data supporting the findings of this study are available within the article and/or its supplemental material.

Supplemental material

Supplemental material for this article is available online.

References

1. Calmette A. The protection of mankind against tuberculosis: being an address before the medico-chirurgical society of Edinburgh. *Edinb Med J* 1922; 29: 93–104.
2. Kremenovic M, Schenk M and Lee DJ. Clinical and molecular insights into BCG immunotherapy for melanoma. *J Intern Med* 2020; 288: 625–640.
3. Morton DL, Mozzillo N, Thompson JF, et al. An international, randomized, phase III trial of bacillus calmette-guerin (BCG) plus allogeneic melanoma vaccine (MCV) or placebo after complete resection of melanoma metastatic to regional or distant sites. *J Clin Oncol* 2007; 25: 8508–8508.
4. Rahmat JN, Esuvaranathan K and Mahendran R. Bacillus Calmette-Guerin induces rapid gene expression changes in human bladder cancer cell lines that may modulate its survival. *Oncol Lett* 2018; 15: 9231–9241.
5. Aaby P, Benn CS, Flanagan KL, et al. The non-specific and sex-differential effects of vaccines. *Nat Rev Immunol* 2020; 20: 464–470.
6. Benn CS, Fisker AB, Rieckmann A, et al. Vaccinology: time to change the paradigm? *Lancet Infect Dis* 2020; 20: e274–e283.
7. Arts RJW, Carvalho A, La Rocca C, et al. Immunometabolic pathways in BCG-induced trained immunity. *Cell Rep* 2016; 17: 2562–2571.
8. Klein BY. Newborn BCG vaccination complemented by boosting correlates better with reduced juvenile diabetes in females, than vaccination alone. *Vaccine* 2020; 38: 6427–6434.
9. Sun J, Furio L, Mecheri R, et al. Pancreatic beta-cells limit autoimmune diabetes via an immunoregulatory antimicrobial peptide expressed under the influence of the gut microbiota. *Immunity* 2015; 43: 304–317.
10. Aronson NE, Santosham M, Comstock GW, et al. Long-term efficacy of BCG vaccine in American Indians and Alaska natives: a 60-year follow-up study. *JAMA* 2004; 291: 2086–2091.
11. Moorlag S, Rodriguez-Rosales YA, Gillard J, et al. BCG Vaccination induces long-term functional reprogramming of human neutrophils. *Cell Rep* 2020; 33: 108387.
12. Cirovic B, de Bree LCJ, Groh L, et al. BCG Vaccination in humans elicits trained immunity via the hematopoietic progenitor compartment. *Cell Host Microbe* 2020; 28: 322–334. e325.
13. Kuhtreiber WM, Tran L, Kim T, et al. Long-term reduction in hyperglycemia in advanced type 1 diabetes: the value of induced aerobic glycolysis with BCG vaccinations. *NPJ Vaccines* 2018; 3: 23.
14. Gofrit ON, Klein BY, Cohen IR, et al. Bacillus calmette-guerin (BCG) therapy lowers the incidence of Alzheimer's disease in bladder cancer patients. *PLoS One* 2019; 14: e0224433.
15. Radford H, Moreno JA, Verity N, et al. PERK Inhibition prevents tau-mediated neurodegeneration in a mouse model of frontotemporal dementia. *Acta Neuropathol* 2015; 130: 633–642.
16. Cabral-Miranda F and Hetz C. Preventing brain aging by the artificial enforcement of the unfolded protein response: future directions. *Neural Regen Res* 2024; 19: 393–394.
17. Zhang M, Liu L, Lin X, et al. A translocation pathway for vesicle-mediated unconventional protein secretion. *Cell* 2020; 181: 637–652. e615.
18. Hetz C, Martinon F, Rodriguez D, et al. The unfolded protein response: integrating stress signals through the stress sensor IRE1alpha. *Physiol Rev* 2011; 91: 1219–1243.
19. Gerakis Y and Hetz C. Emerging roles of ER stress in the etiology and pathogenesis of Alzheimer's disease. *FEBS J* 2018; 285: 995–1011.
20. Ghemrawi R and Khair M. Endoplasmic reticulum stress and unfolded protein response in neurodegenerative diseases. *Int J Mol Sci* 2020; 21: 6127.
21. Tian X, Zhang S, Zhou L, et al. Targeting the integrated stress response in cancer therapy. *Front Pharmacol* 2021; 12: 747837.
22. Lotem M, Machlenkin A, Hamburger T, et al. Autologous melanoma vaccine induces antitumor and self-reactive immune responses that affect patient survival and depend on MHC class II expression on vaccine cells. *Clin Cancer Res* 2009; 15: 4968–4977.
23. Lotem M, Merims S, Frank S, et al. Adjuvant autologous melanoma vaccine for macroscopic stage III disease: survival, biomarkers, and improved response to CTLA-4 blockade. *J Immunol Res* 2016; 2016: 8121985.
24. Claman HN and Miller SD. Requirements for induction of T cell tolerance to DNFB: efficiency of membrane-associated DNFB. *J Immunol* 1976; 117: 480–485.
25. Schwartz M. Can immunotherapy treat neurodegeneration? *Science* 2017; 357: 254–255.
26. Hoozemans JJ, van Haastert ES, Nijholt DA, et al. Activation of the unfolded protein response is an early event in Alzheimer's and Parkinson's disease. *Neurodegener Dis* 2012; 10: 212–215.
27. Nijholt DA, van Haastert ES, Rozemuller AJ, et al. The unfolded protein response is associated with early tau pathology in the hippocampus of tauopathies. *J Pathol* 2012; 226: 693–702.
28. Hoozemans JJ, Veerhuis R, Van Haastert ES, et al. The unfolded protein response is activated in Alzheimer's disease. *Acta Neuropathol* 2005; 110: 165–172.
29. Fritsch RM, Schneider G, Saur D, et al. Translational repression of MCL-1 couples stress-induced eIF2 alpha phosphorylation to mitochondrial apoptosis initiation. *J Biol Chem* 2007; 282: 22551–22562.
30. Rojas M, Gingras AC and Dever TE. Protein phosphatase PP1/GLC7 interaction domain in yeast eIF2gamma bypasses targeting subunit requirement for eIF2alpha dephosphorylation. *Proc Natl Acad Sci U S A* 2014; 111: E1344–E1353.

31. Akatsuka Y, Nishida T, Kondo E, et al. Identification of a polymorphic gene, BCL2A1, encoding two novel hematopoietic lineage-specific minor histocompatibility antigens. *J Exp Med* 2003; 197: 1489–1500.
32. Kausalya S, Somogyi R, Orlofsky A, et al. Requirement of A1-a for bacillus Calmette-Guerin-mediated protection of macrophages against nitric oxide-induced apoptosis. *J Immunol* 2001; 166: 4721–4727.
33. Martinon F and Glimcher LH. Regulation of innate immunity by signaling pathways emerging from the endoplasmic reticulum. *Curr Opin Immunol* 2011; 23: 35–40.
34. Rozpedek W, Pytel D, Poplawski T, et al. Inhibition of the PERK-dependent unfolded protein response signaling pathway involved in the pathogenesis of Alzheimer's disease. *Curr Alzheimer Res* 2019; 16: 209–218.
35. Nwosu GO, Powell JA and Pitson SM. Targeting the integrated stress response in hematologic malignancies. *Exp Hematol Oncol* 2022; 11: 94.
36. Kim JI, Kaufman RJ, Back SH, et al. Development of a reporter system monitoring regulated intramembrane proteolysis of the transmembrane bZIP transcription factor ATF6alpha. *Mol Cells* 2019; 42: 783–793.
37. Yoshida H, Matsui T, Yamamoto A, et al. XBP1 mRNA is induced by ATF6 and spliced by IRE1 in response to ER stress to produce a highly active transcription factor. *Cell* 2001; 107: 881–891.
38. Yamamoto K, Sato T, Matsui T, et al. Transcriptional induction of mammalian ER quality control proteins is mediated by single or combined action of ATF6alpha and XBP1. *Dev Cell* 2007; 13: 365–376.
39. Kuhtreiber WM, Takahashi H, Keefe RC, et al. BCG Vaccinations upregulate Myc, a central switch for improved glucose metabolism in diabetes. *iScience* 2020; 23: 101085.
40. Shpilsky GF, Takahashi H, Aristarkhova A, et al. Bacillus Calmette-Guerin 's beneficial impact on glucose metabolism: evidence for broad based applications. *iScience* 2021; 24: 103150.
41. Calfon M, Zeng H, Urano F, et al. IRE1 Couples endoplasmic reticulum load to secretory capacity by processing the XBP-1 mRNA. *Nature* 2002; 415: 92–96.
42. Amin-Wetzel N, Saunders RA, Kamphuis MJ, et al. A J-protein co-chaperone recruits BiP to monomerize IRE1 and repress the unfolded protein response. *Cell* 2017; 171: 1625–1637. e1613.
43. Lanzillotta C, Zuliani I, Tramutola A, et al. Chronic PERK induction promotes Alzheimer-like neuropathology in down syndrome: insights for therapeutic intervention. *Prog Neurobiol* 2021; 196: 101892.
44. Cabral-Miranda F, Tamburini G, Martinez G, et al. Unfolded protein response IRE1/XBP1 signaling is required for healthy mammalian brain aging. *EMBO J* 2022; 41: e111952.
45. Ismael S, Wajidunnisa, Sakata K, et al. ER Stress associated TXNIP-NLRP3 inflammasome activation in hippocampus of human Alzheimer's disease. *Neurochem Int* 2021; 148: 105104.
46. Moreno JA, Radford H, Peretti D, et al. Sustained translational repression by eIF2alpha-P mediates prion neurodegeneration. *Nature* 2012; 485: 507–511.
47. Li G, Liang R, Lian Y, et al. Circ_0002945 functions as a competing endogenous RNA to promote abeta(25-35)-induced endoplasmic reticulum stress and apoptosis in SK-N-SH cells and human primary neurons. *Brain Res* 2022; 1785: 147878.
48. Montibeller L and de Belleroche J. Amyotrophic lateral sclerosis (ALS) and Alzheimer's disease (AD) are characterised by differential activation of ER stress pathways: focus on UPR target genes. *Cell Stress Chaperones* 2018; 23: 897–912.
49. van der Meer JW, Joosten LA, Riksen N, et al. Trained immunity: a smart way to enhance innate immune defence. *Mol Immunol* 2015; 68: 40–44.
50. Nguyen HD, Chatterjee S, Haarberg KM, et al. Metabolic reprogramming of alloantigen-activated T cells after hematopoietic cell transplantation. *J Clin Invest* 2016; 126: 1337–1352.
51. Sarnow P. Translation of glucose-regulated protein 78/immunoglobulin heavy-chain binding protein mRNA is increased in poliovirus-infected cells at a time when cap-dependent translation of cellular mRNAs is inhibited. *Proc Natl Acad Sci U S A* 1989; 86: 5795–5799.
52. Kim JI, Zhu D, Barry E, et al. Intravesical Bacillus Calmette-Guerin treatment is inversely associated with the risk of developing Alzheimer disease or other dementia among patients with non-muscle-invasive bladder cancer. *Clin Genitourin Cancer* 2021; 19: e409–e416.
53. Klinger D, Hill BL, Barda N, et al. Bladder cancer immunotherapy by BCG is associated with a significantly reduced risk of Alzheimer's disease and Parkinson's disease. *Vaccines (Basel)* 2021; 9: 491.
54. Makrakis D, Holt SK, Bernick C, et al. Intravesical BCG and incidence of Alzheimer disease in patients with bladder cancer: results from an administrative dataset. *Alzheimer Dis Assoc Disord* 2022; 36: 307–311.
55. Weinberg MS, Zafar A, Magdamo C, et al. Association of BCG vaccine treatment with death and dementia in patients with non-muscle-invasive bladder cancer. *JAMA Netw Open* 2023; 6: e2314336.
56. Park G, Xu K, Chea L, et al. Neurodegeneration risk factor, EIF2AK3 (PERK), influences tau protein aggregation. *J Biol Chem* 2023; 299: 102821.
57. van Dijk A, Anten J, Bakker A, et al. Innate immune training of human macrophages by cathelicidin analogs. *Front Immunol* 2022; 13: 777530.
58. Brook B, Harbeson DJ, Shannon CP, et al. BCG vaccination-induced emergency granulopoiesis provides rapid protection from neonatal sepsis. *Sci Transl Med* 2020; 12: eaax4517.
59. Sanchez-Ramos J, Cimino C, Avila R, et al. Pilot study of granulocyte-colony stimulating factor for treatment of Alzheimer's disease. *J Alzheimers Dis* 2012; 31: 843–855.

60. Wang SM, Kang DW, Kim HJ, et al. Neuroplastic and procognitive effects of granulocyte colony stimulating factor in healthy adults: a pilot study. *Psychiatry Investig* 2023; 20: 984–990.

61. Savickiene J, Treigyte G, Vistartaite G, et al. C/EBPalpha and PU.1 are involved in distinct differentiation responses of acute promyelocytic leukemia HL-60 and NB4 cells via chromatin remodeling. *Differentiation* 2011; 81: 57–67.